Interpenetrating PAA-PEDOT Conductive Hydrogels for Flexible Skin Sensors

Fanfan Fu,[1] Jilei Wang,[1] Jing Yu[1]*

*[1]School of Materials Science and Engineering, Nanyang Technological University, 639798, Singapore. *E-mail: yujing@ntu.edu.sg (J. Yu)*

ABSTRUCT: Conductive hydrogels are promising material candidates in artificial skin and muscles, flexible and implantable bioelectronics, and tissue engineering. However, it is still a challenge to formulate hydrogels with high electrical conductivity without compromising their physicochemical properties. Herein, we report an interpenetrating poly(acrylic acid)-poly (3,4-ethylenedioxythiophene) (PAA-PEDOT) hydrogel with high electrical conductivity and good stretchability. A second PEDOT hydrogel network is electrochemically polymerized into an existing PAA hydrogel network. The interpenetrating hydrogel can be readily prepared and can be integrated into epidermal flexible electronic devices for the real-time, on-body detection of various ions in sweat. The interpenetrating PAA-PEDOT conductive hydrogel has the potential to be an important building material for various flexible electronic devices for personalized healthcare.

Introduction

Flexible bioelectronic devices interfacing with human body and organ have great potentials in various applications in the realm of personalized health monitoring,[1] including sweat sensors,[2] sensors for electrophysiological signals[3-5] (such as electrocardiogram (ECG), electromyography (EMG), and electroencephalography (EEG)), and electronic skin.[6-9] Currently, the fabrication of bioelectronic devices mostly relies on inorganic materials with appropriate electrical conductivity, such as silicon and metals.[10-13] These traditional inorganic materials suffer from some inherent limitations due to their different chemical and mechanical properties from biological tissue, leading to serious problems at the device-tissue interface such as tissue inflammation, non-conformal contact between the devices and human skin/tissue, and unreliable signal collection.[14-16] Hydrogels, with high water content, similar mechanical properties to human tissue, and good biocompatibility, is an ideal class of materials for bioelectronic devices.[17-19] However, the electrical conductivity of most hydrogels is much lower than that of inorganic materials, which greatly limits the application of hydrogels in bioelectronics.[20] Developing conductive hydrogels with good biocompatibility and high electrical capability is of great value for next-generation flexible bioelectronic devices.[21-25]

Conductive hydrogels are a good class of materials for replacing traditional inorganic materials for bioelectronic devices owing to their porous structure, tunable chemical and mechanical properties, and suitable electronical performance.[26-29] The porous structure of conductive hydrogels with high-water content can provide an extracellular matrix (ECM)-like environment that allows for the transport of various molecules, thereby facilitating the exchange of biomolecules and biomarkers across interfaces.[30-32] By tuning the chemical structure, hydrogels can provide mechanical and chemical properties that match to these of human tissue.[33,

[34] In comparison to the traditional inorganic electrode materials, conductive hydrogels based on conducting polymers such as poly (3,4-ethylenedioxythiophene) (PEDOT), polyaniline (PANI), and polypyrrole (PPy) have prominent advantages, including good biocompatibility and low electrical impedance.[35-39]

The main challenge in the field of developing of conductive hydrogels for bioelectronics is to achieve reasonably high conductivity, while not sacrificing their physicochemical properties, such as high toughness, good stretchability, and good biocompatibility.[40] Hydrogels composed by conductive polymers such as PEDOT inherit their conductivity from the conjugated π bond of the conductive polymers.[41-43] However, the conjugated structures are inherently rigid, which results in poor mechanical properties. A common strategy to prepare conductive hydrogels with good mechanical properties is to form an interpenetrating conductive hydrogel network by in-situ polymerization of a conductive polymer network within an existed non-conductive hydrogel matrix. However, hydrogels prepared by such method often suffer from low electrical conductivity.[26] Another common method for improving the conductivity of the hydrogels is to add conductive fillers into the hydrogel matrix. Different materials, including carbon nanotubes,[44-46] graphene,[47, 48] and metal nanoparticles/wires,[49-51] have been used as fillers to increase the conductivity of the hydrogels. In order to achieve good conductivity, high content of conductive fillers needs be used, which affects the mechanical properties as well as the biocompatibility of the hydrogels.[52]

In this work, we develop a highly conductive and stretchable interpenetrating PAA-PEDOT hydrogel. By in-situ electrochemical polymerization of EDOT monomer in an existing PAA hydrogel network, a dense PEDOT network with high conductivity is introduced into a PAA matrix, forming an interpenetrating PAA-PEDOT hydrogel (**Fig. 1**). The interpenetrating PAA-PEDOT

hydrogel, molded with additional surface microstructures, can withstand external stretch without compromising its conductivity. Taking advantage of the interpenetrating PAA-PEDOT hydrogel, hydrogel-based electrodes can be fabricated for the detection of ionic species such as Na^+ and K^+ ions in solution. The hydrogel electrodes can be incorporated into flexible epidermal sensors for the real-time, on-body detection of various ions in the sweat.

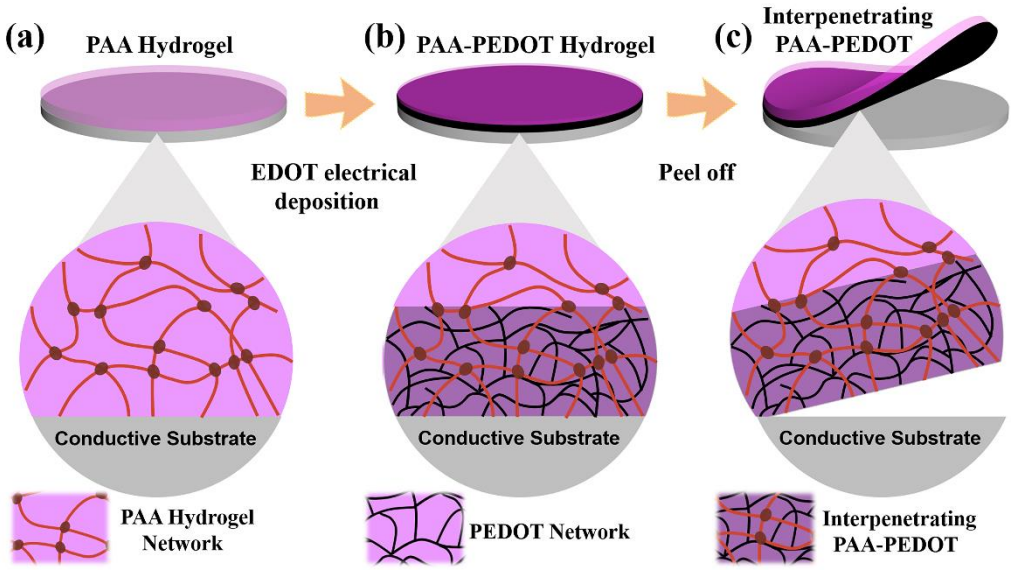

Fig. 1. Schematic diagram of the preparation process of interpenetrating PAA-PEDOT hydrogel.

Result and discussion

We fabricated the PAA-PEDOT hydrogel with high conductivity by in situ polymerization of 3,4-ethylenedioxythiophene (EDOT) monomer into an existing PAA hydrogel matrix. A PAA hydrogel was first synthesized on an indium-tin-oxide glass (ITO) template with a thickness of about 0.3 mm (**Fig. 2a**). The ITO glass with the PAA hydrogel was then immersed into a solution consisted of EDOT monomers. The EODT monomers gradually diffused into the PAA hydrogel and enriched at the PAA-ITO interface. After 10 mins, a voltage of 1.5V was applied to the ITO surface to introduce the electrochemical polymerization of the EDOT monomers into a PEDOT

network at the PAA-ITO interface, resulting in an interpenetrating PAA-PEDOT hydrogel (**Fig. 2b**). The PAA hydrogel network serves as a supporting scaffold to the electropolymerized PEDOT network. The crosslink density of the PAA hydrogel is one of the main factors that control the formation of the PEDOT hydrogel network. At low crosslink densities, the PAA hydrogel matrix is too weak to serve as a scaffold for the growth of the PEDOT network (**Fig. S1a**), whereas a high crosslink density PAA hydrogel will limit the in-situ electrochemical polymerization of PEDOT due to the impaired diffusion of the EDOT monomers in a dense polymer network (**Fig. S1c**). After a series of optimization, we identified that a pre-gel solution of 30wt% acrylic acid (AA) monomer would result in consistent PAA-PEDOT interpenetrating hydrogel with balanced mechanical and conductive properties (**Fig. S1b**). The formed PEDOT-PAA hydrogel showed a decreased contact angle than the pure PAA hydrogel (**Fig. 2a and b**) due to the interpenetrating PEDOT network.

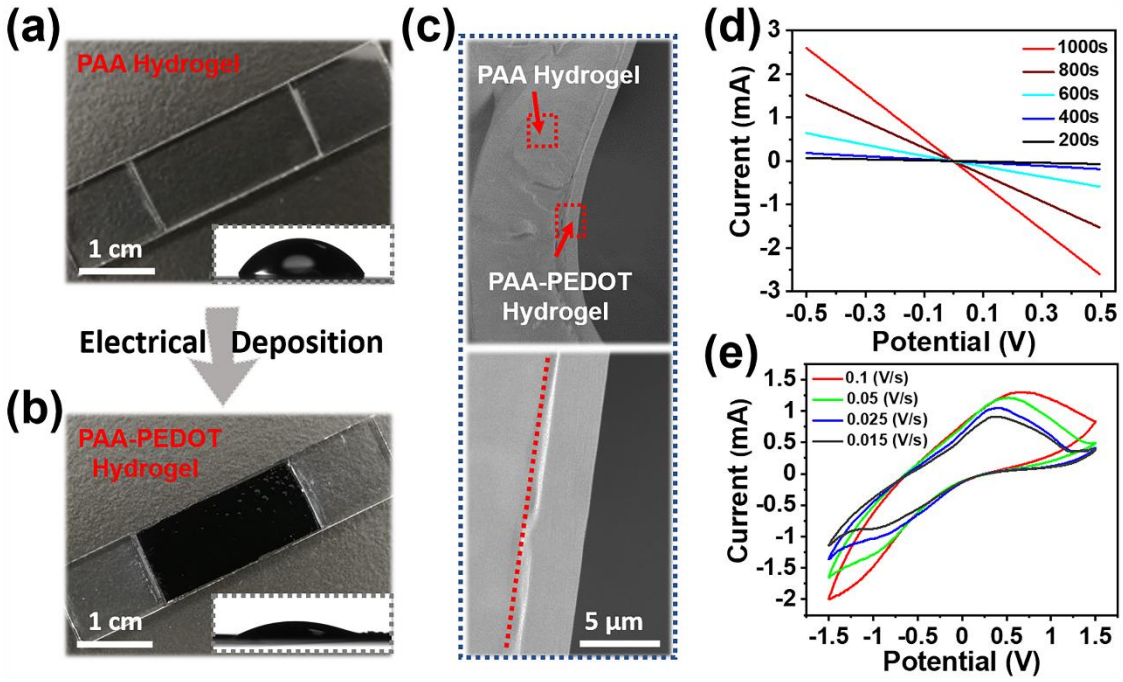

Fig. 2. Preparation process of the interpenetrating PAA-PEDOT hydrogel. Images of a PAA hydrogel (a) and a PAA-PEDOT hydrogel (b) on ITO glass. The insets of (a) and (b) are the contact angle images of the PAA hydrogel and PAA-PEDOT hydrogel, respectively. (c) SEM image of the

section of a PAA-PEDOT hydrogel. (d) Measured current-voltage curves of the PAA-PEDOT hydrogel with different electronical deposition times. (e) cyclic voltammograms (CV) measurements of the PAA-PEDOT hydrogel at different scan rates.

The PAA-PEDOT hydrogels show a Janus structure (**Fig. 2c**) with one layer consisting mostly of PAA and the other layer being the interpenetrating PAA-PEDOT hydrogel. Taking advantage of the hydrogen bond forming ability of the carboxyl groups in the PAA hydrogel layer, the resulting hydrogel has strong adhesion on different surfaces,[54, 55] such as attaching to the surface of the metal, glass, and human skin (**Fig. S2**). As the polymerization time increased, the concentrated PEDOT cluster formed on the surface of the hydrogel became denser (**Fig. S3**). The current-voltage curves of the PAA-PEDOT hydrogel (**Fig. 2d**) show that as the polymerization time increases, the resistance of the formed PAA-PEDOT hydrogel decreases. By controlling the electrochemical polymerization time (~15 mins), we obtained highly conductive PAA-PEDOT hydrogel with a resistance of ~200 Ω for a 1 cm by 1 cm hydrogel. Due to the difficulty of obtaining accurate thickness of the PAA-PEDOT interpenetrating layer, we were not able to measure the accurate conductivity of the hydrogel. The electrochemical property of the PAA-PEDOT hydrogel was measured by cyclic voltammograms (CV). The CV curves of PAA-PEDOT hydrogel show a PEDOT oxidation peak at 0.3V and a reduction peak around −0.9 V at different scan rates, and the current increases with the increase of the scan rate (**Fig. 2e**), which is highly in line with the studies of PEDOT polymer and its derivative.[56]

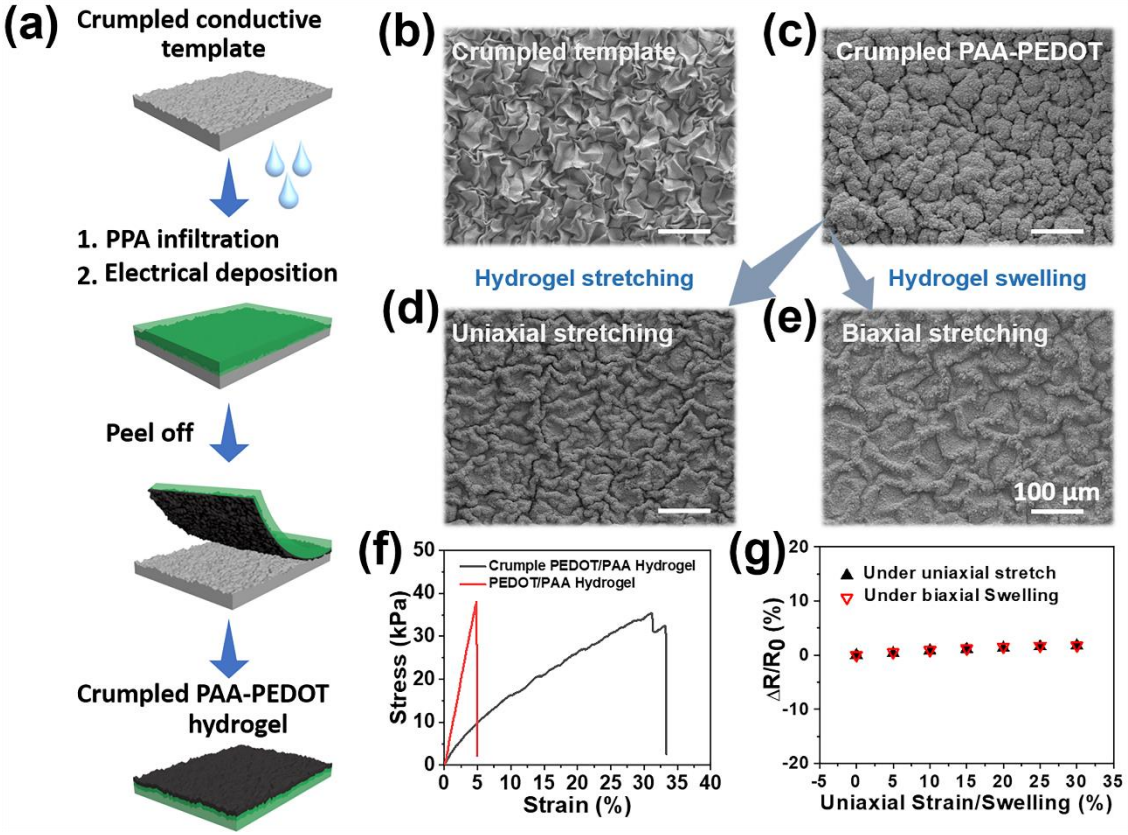

Fig. 3. Preparation process of crumpled PAA-PEDOT hydrogels. (a) A schematic preparation process of the crumpled PAA-PEDOT hydrogels. SEM image of (b) a crumpled rGO/Pt template. SEM images of the crumpled PAA-PEDOT hydrogel under (c) normal, (d) uniaxial stretching and (e) biaxial stretching conditions. (f) The typical stress-strain curves of a flat PAA-PEDOT hydrogel and a crumpled PAA-PEDOT hydrogel. (g) The change of resistance ($\Delta R/R_0$) of the crumpled PAA-PEDOT hydrogel as functions of tensile strain and biaxial hydrogel swelling. Scale bars are 100 μm in (b-e).

To make the PAA-PEDOT hydrogel stretchable, a conductive crumpled rGO/Pt substrate was used as a template for the synthesis of the interpenetrating PAA-PEDOT hydrogel (**Fig. 3a**). To obtain the crumpled rGO/Pt substrate, a polystyrene (PS) shrink film, which can form wrinkle structures upon heating was used as a template for preparing a rGO/Pt film. GO solution was first casted on the surface of the PS film to form a closely packed multilayer structure, followed by heat

shrinkage, hydrogen iodide (HI) reduction, and Pt sputtering process to form the rGO/Pt template (**Fig. 3b and Fig. S4**). Due to the crumpled template, the fabricated PAA-PEDOT hydrogel also showed wrinkle surface structure and could undergo a 30% strain uniaxial stretching and biaxial swelling (30% strain) processes without destroying its microstructures (**Fig. 3c-e**). The Yong's modulus of the crumpled PAA-PEDOT hydrogel is 226 KPa, which is smaller than that of the flat PAA-PEDOT hydrogel (788 KPa) (**Fig. 3f**). However, the flat PAA-PEDOT hydrogel can only hold approximately 5% strain before mechanical failure while the crumpled PAA-PEDOT can withstand a 30% strain while reaching similar failure stress. More importantly, the crumpled PAA-PEDOT hydrogel can maintain a stable electrical resistance under stretching. The $\Delta R/R_0$ of the crumpled PAA-PEDOT hydrogel has negligible change under up to 30% strain of uniaxial stretching or biaxial swelling (**Fig. 3g**). Such stable resistance indicates that the crumpled PAA-PEDOT hydrogel can be used as an electrode material in various flexible bioelectronic devices.

To further exploit the potential of using the interpenetrating PAA-PEDOT hydrogel as the electrode materials for flexible electronic devices, we designed the PAA-PEDOT hydrogel-based sensor as the working electrode for the detection of various ions in solution. In brief, the pregel AA solution was first spread on a conductive substrate and exposed to UV light (365 nm, 200 s) with a photomask templates forming patterned hydrogel. The patterned hydrogel was then immersed in a solution with EDOT monomers to form the PAA-PEDOT hydrogel electrode via electrochemical deposition. A silver/silver chloride (Ag/AgCl) electrode was used as the reference electrode. Ion selective membranes were coated on the hydrogel electrodes by solution casting to obtain the electrochemical sensors for detecting Na^+ and K^+ ions. The performance of each hydrogel sensor was monitored separately by using the open circuit potentials (OCPT) method. Solutions with various concentrations of Na^+(10-160 mM) and K^+ (1-16 mM) were used to

evaluate the hydrogel's sensing ability. The ranges of concentration of two ions were chosen based on the physiological range of concentrations of the ions in human sweat. As showing in **Fig. 4a** and **b**, the PAA-PEDOT hydrogel-based ion-selective sensors show near-Nernstian behavior with sensitivities of 56.2 mV and 42.5 mV per decade of concentration for Na^+ and K^+ sensors, respectively.

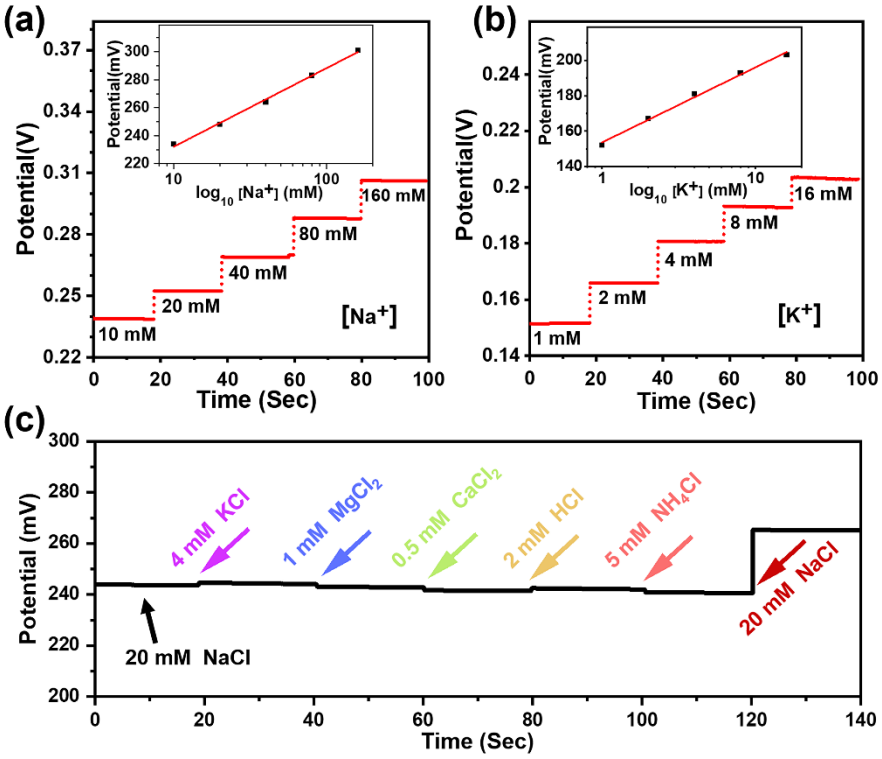

Fig. 4. PAA-PEDOT hydrogel-based Na^+ and K^+ sensors. (a-b) The open circuit potential responses of the sodium (a) and potassium (b) sensors in different concentrations of NaCl and KCl solutions. Insets in a-b are the corresponding calibration plots of the ionic sensors. (c) The selectivity performance of Na^+ sensor in different ionic solutions.

The selectivity of the hydrogel-based ion sensors is crucial in practical applications such as detection the concentrations of different ions in the sweat. To test the selectivity of our hydrogel-based Na^+ sensor, the sensor was sequentially immersed into solutions with 4 mM K^+, 1 mM Mg^{2+}, 0.5 mM Ca^{2+}, 2 mM H^+, and 5 mM NH_4^+, while the open circuit potential of the sensor was

monitored. The results showed that the presence of nontarget ions only caused very small interference potential (±3 mV) to the response of the hydrogel sensor. Upon adding a solution containing 20 mM NaCl, a jump of the surface potential of ~20 mV was recorded, demonstrating the excellent selectivity of our Na^+ sensor (**Fig. 4c**). The selectivity of the K^+ sensor was evaluated similarly (**Fig. S5**).

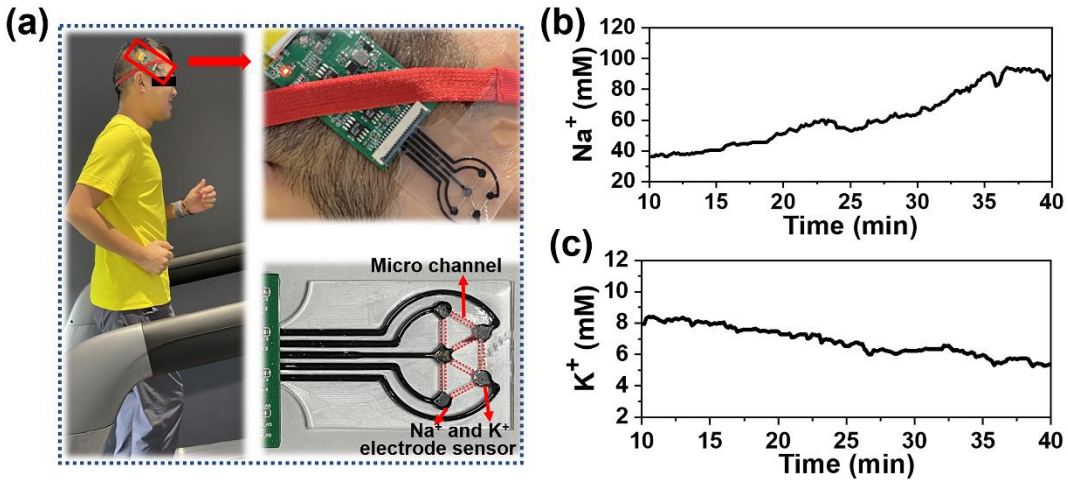

Fig. 5. Real-time perspiration analysis during a running exercise. (a) Photographs of a subject wearing a sweat sensor during running exercise. (b, c) the real-time data chart of the Na^+ (b) and K^+ (c) concentrations in the on-body sweat samples with the readings of the PAA-PEDOT based sensor during the running exercise.

The PAA-PEDOT conductive hydrogel can serve as an alternative electrode material for epidermal flexible electronic devices. To demonstrate its potential for such applications, we fabricated a microfluidic sweat sensor for real-time monitoring of Na^+ and K^+ concentrations in human sweat. We designed a PDMS chip consisting of the designed electrode area, circuit area and the sweat transportation microchannels (**Fig. 5**). The sweat transportation microchannels connect to each electrode, endowing the same working conditions for all the ion sensors. The PAA-PEDOT hydrogel modified with Na^+ and K^+-selective membranes was used as the sensors. The microfluidic sweat sensor was connected to a printed circuit board for the real-time monitoring of

human sweat (**Fig. 5a**). Before being used for the on-body detection of sweat, the integrated device was tested in solutions containing Na^+ ion (50 mM, 120 mM) and K^+ ion (5 mM, 8 mM) to determine the stability of the instrument (**Fig. S6**). In a period of 30 minutes, the fluctuation range of such integrated device is within 12.2 and 15.1% for Na^+ (50 mM) and K^+ (5 mM), respectively. To further test the stability of the fabricated hydrogel sensors, we performed a multicycle stability test for 2 hours (12 cycles) using Na^+ and K^+ solutions (**Fig. S7**), and our hydrogel sensors provided consistent read-outs during the whole multicycle test.

The integrated PAA-PEDOT hydrogel based sweat sensor was fixed on the forehead of a subject for the real-time sweat monitoring during a running exercise (6 minutes/km). During the running exercise period, the data collection and recording were performed when perspiration phenomenon continued to appear and visually observed. The concentration of Na^+ gradually increased as a function of excising time (**Fig. 5b**), while the concentration K^+ of slowly decreased during the period of the exercise (**Fig. 5c**). These results were consistent with the previous studies,[6][57-59] indicating that such PAA-PEDOT hydrogel-based sweat sensor can be used for on-body, real-time monitoring of the concentrations of various ions in the human sweat. This hydrogel-based sensor enables the quantitative analysis of the concentrations of sodium and potassium ions in real-time. Such information is critical for monitoring the hydration state of the body during exercise.

Conclusion

In summary, we develop a flexible and stretchable interpenetrating PAA-PEDOT hydrogel with good electrical conductivity. By incorporating additional surface microstructures, the interpenetrating PAA-PEDOT hydrogel can withstand 30% external stretching without

compromising its conductivity. Taking advantage of these merits, the developed PAA-PEDOT hydrogel can be used to fabricate hydrogel-based electrochemical sensors, which can be used as ion sensors for epidermal sweat sensors, such as Na^+, and K^+. The interpenetrating PAA-PEDOT conductive hydrogel can serve as an important electrode material for flexible electronic devices for personalized healthcare, including monitoring the important chemical biomarkers in the sweat such as ions, glucose, and lactic acid, measuring various electrophysiological signals (EEG, ECG, and EMG), as well as in vivo nerve signal recording and stimulation.

Experimental section

Materials and Methods.

Acrylic acid (AA), N,N-Methylene-bisacrylamide (BIS), and 2-hydroxy-2-methyl-1-phenyl-1-propanone (HMPP), and silver conductive paint were purchased from Sigma-Aldrich. 3,4-ethylenedioxythiophene (EDOT), Lithium perchlorate ($LiClO_4$), Polyvinyl butyral (PVB), Pluronic F-127, Bis (2-ethylehexyl) sebacate (DOS), Sodium tetrakis [3,5-bis(trifluoromethyl)phenyl] borate (Na-TFPB), High-molecular-weight polyvinyl chloride (PVC), poly-(sodium 4-styrenesulfonate) (NaPSS), Iron (III) chloride ($FeCl_3$), and Acetonitrile (CH_3CN) were obtained from Sigma-Aldrich. Graphene oxide (GO) aqueous solution (10 mg mL^{-1}, flake size 50–200 nm) were purchased from XF NANO, Nanjing, China. Polystyrene (PS) heat shrink films were obtained from USA (Grafix). Polydimethylsiloxane (PDMS) was purchased from USA (Dow Corning). Deionized water used in all experiments was purified by using a purification system (Thermo Scientific) with resistivity higher than 18 MΩ cm.

Hydrogel characterization

Cyclic voltammetry (CV) was performed on the PAA-PEDOT hydrogel by using a potentiostat/galvanostat (CHI 660) with the scan rates of 15 to 100 mVs^{-1}. Electrical conductivity of the conductive hydrogel was measured using a Keithley 2650 digital multimeter. Scanning electron microscope (SEM) images of the hydrogel samples were taken by field-emission scanning electron microscopy (FESEM, JEOL JSM-7600F, 5 kV) with a layer of gold sputtering to enhance image contrasts.

Preparation of the PAA-PEDOT hydrogel.

The monomer of AA and crosslinker BIS were first mixed (with a mass ratio of 30:1) and dissolved (w. 30%) in deionized water. To from the PAA hydrogel, a photoinitiator HMPP (1%, v/v) was added into the monomer and crosslinker pre-gel solution. The PAA hydrogel was obtained by exposing the pre-gel solution (spread on substrate) with UV light (365 nm, 30s). To prepare the interpenetrating PAA-PEDOT hydrogel, EDOT (0.05 mol/L) monomer was dissolved in acetonitrile/water and in-situ polymerized by electrochemical deposition. Briefly, a PAA hydrogel (with a thickness of ~300 μm) was first formed on conductive ITO glass substrate. Subsequently, the PAA/ITO film was immersed in an acetonitrile/water (v/v 4:1) solution containing EDOT (0.05M) and $LiClO_4$ (0.1M). EDOT was electrochemically deposited on the interface between hydrogel and conductive substrate (1.35 V vs Ag/AgCl, 10 min) to form an interpenetrating PAA-PEDOT hydrogel. Finally, the obtained hydrogel was peeled off from the ITO glass by using the electrochemical elastic actuation property of PEDOT (±0.5 V vs Ag/AgCl). In addition, the crumple structured interpenetrating PAA-PEDOT hydrogel was obtained by using a crumple rGO/Pt template. The PAA-PEDOT hydrogel with different patterns can be prepared by using UV mask templates.

Fabrication of the PPA-PEDOT based electrochemical sensor.

Ion selective (Na^+ and K^+) membrane used for electrode modification were prepared according to reported literature.[6, 53] The Na^+ selective membrane mixture consisted of Na ionophore X (1%, w/w), Na-TFPB (0.5%, w/w), PVC (33.0 %, w/w), and DOS (65.5 %, w/w). The mixture was dissolved in tetrahydrofuran (0.15 mg/μL) to form the Na^+ membrane solution. The K^+ selective membrane mixture consisted of valinomycin (2% w/w), NaTPB (0.5%), PVC (33.0% w/w), and DOS (64.5% w/w). The mixture was dissolved in cyclohexanone (0.3 mg/μL) to form K^+ membrane solution. All the solutions were stored at 4 °C. The ion-selective membrane solution (10 μL) was drop-casted on the surface of corresponding electrode to form the Na^+ and K^+ selective membranes, respectively. The common reference electrode was prepared by casting PVB solution (10 μL) on the surface of Ag/AgCl electrode, followed by drying overnight at room temperature. The PVB solution used for Ag/AgCl reference electrode modification consisted of PVB (79.0 mg), NaCl (50 mg), F127 (36.2 mg), multiwall carbon nanotubes (0.2 mg), and 1 mL methanol.

On body sweat chip fabrication.

For the integration of an on body sweat chip, the hydrogel electrode array was first fabricated via photolithography. In brief, the PAA pre-gel was first laid flat on the surface of the conductive substrate, and then cured with the UV light with a photomask to obtain the hydrogel pattern. The EDOT monomer was electrochemically deposited into the patterned PAA hydrogel to form an interpenetrating PAA-PEDOT hydrogel electrode array. The hydrogel electrode array was then transferred and integrated into a microfluidic PDMS chip for sweat collection. Finally, the electrode array was coated with ion selective membranes or Ag/AgCl solution to form the PAA-PEDOT conductive hydrogel based sweat sensor. To evaluate the stability of hydrogel-based sensor, the integrated device was tested in solutions of Na^+ (50 mM, 120 mM) and K^+ (50 mM, 120 mM), and realized the multi-cycle stability test by switching ion solutions.

Conflicts of interest

The authors declare no competing financial interest.

Acknowledgements

F. F. Fu, J. L. Wang, and J. Yu acknowledge the AME programmatic funding scheme of Cyber Physiochemical Interfaces (CPI) project #A18A1b0045 and Singapore Ministry of Education Academic Research Fund Tier 1 RT 06/20.

Author information

Corresponding authors

Jing Yu - School of Materials Science and Engineering, Nanyang Technological University 639798, Singapore; orcid.org/0000-0002-4288-951X.

*Email: yujing@ntu.edu.sg

Others Author

Fanfan Fu - School of Materials Science and Engineering, Nanyang Technological University 639798, Singapore; orcid.org/0000-0002-4443-9846;

Jilei Wang - School of Materials Science and Engineering, Nanyang Technological University 639798, Singapore; orcid.org/0000-0002-0950-0971;

Reference

1. Y. J. Ma, Y. C. Zhang, S. S. Cai, Z. Y. Han, X. Liu, F. L. Wang, Y. Cao, Z. H. Wang, H. F. Li, Y. H. Chen and X. Feng, *Adv. Mater.,* 2020, **32**, 1902062.
2. W. Y. He, C. Y. Wang, H. M. Wang, M. Q. Jian, W. D. Lu, X. P. Liang, X. Zhang, F. C. Yang and Y. Y. Zhang, *Sci. Adv.*, 2019, **5**, 0649.

3. F. F. Fu, J. L. Wang, H. B. Zeng and J. Yu, *ACS Materials Lett.*, 2020, **2**, 1287-1301.

4. A. Moin, A. Zhou, A. Rahimi, A. Menon, S. Benatti, G. Alexandrov, S. Tamakloe, J. Ting, N. Yamamoto, Y. Khan, F. Burghardt, L. Benini, A. C. Arias and J. M. Rabaey, *Nat. Electron.,* 2020, **4**, 54-63.

5. H. Yang, S. B. Ji, I. Chaturvedi, H. R. Xia, T. Wang, G. Chen, L. Pan, C. J. Wan, D. Qi, Y.-S. Ong and X. D. Chen, *ACS Materials Lett*., 2020, **2**, 478-484.

6. W. Gao, S. Emaminejad, H. Y. Y. Nyein, S. Challa, K. Chen, A. Peck, H. M. Fahad, H. Ota, H. Shiraki, D. Kiriya, D. H. Lien, G. A. Brooks, R. W. Davis and A. Javey, *Nature*, 2016, **529**, 509-514.

7. W. Gao, H. Ota, D. Kiriya, K. Takei and A. Javey, *Acc. Chem. Res.,* 2019, **52**, 523-533.

8. C. Y. Wang, K. L. Xia, Y. Y. Zhang and D. L. Kaplan, *Acc. Chem. Res.,* 2019, **52**, 2916-2927.

9. G. Li, D. Chen, C. L. Li, W. X. Liu and H. Liu, *Adv. Sci.*, 2020, **7**, 2000154.

10. D. R. Wang, Y. K. Zhang, X. Lu, Z. J. Ma, C. Xie and Z. J. Zheng, *Chem. Soc. Rev.,* 2018, **47**, 4611-4641.

11. T. Someya, Z. N. Bao and G. G. Malliaras, *Nature*, 2016, **540**, 379-385.

12. Y. H. Chen, S. Y. Lu and X. Feng, 2017 IEEE International Electron Devices Meeting (IEDM), San Francisco, CA.

13. H. Chen, F. Zhu, K. I. Jang, X. Feng, J. A. Rogers, Y. H. Zhang, Y. G. Huang and Y. J. Ma, *J. Mech. Phys. Solids*, 2018, **120**, 199−207.

14. S. Loffler, K. Melican, K. P. R. Nilsson and A. Richter-Dahlfors, *J. Intern. Med.,* 2017, **282**, 24-36.

15. J. W. Salatino, K. A. Ludwig, T. D. Y. Kozai and E. K. Purcell, *Nat. Biomed. Eng.,* 2017, **1**, 862-877.

16. D. T. Simon, E. O. Gabrielsson, K. Tybrandt and M. Berggren, *Chem. Rev.*, 2016, **116**, 13009-13041.

17. H. Yuk, B. Y. Lu and X. H. Zhao, *Chem. Soc. Rev.*, 2019, **48**, 1642-1667.

18. J. Deng, H. Yuk, J. J. Wu, C. E. Varela, X. Y. Chen, E. T. Roche, C. F. Guo and X. H. Zhao, *Nat. Mater.,* 2021, **20**, 229-236.

19. Z. W. Wang, Y. Cong and J. Fu, *J. Mater. Chem. B*, 2020, **8**, 3437-3459.

20. D. Gao, K. Parida and P. S. Lee, *Adv. Funct. Mater.*, 2020, **30**, 1907184.

21. Y. Ohm, C. F. Pan, M. J. Ford, X. N. Huang, J. H. Liao and C. Majidi, *Nat. Electron.*, 2021, https://doi.org/10.1038/s41928-021-00545-5.

22. X. Y. Zhang, J. S. Chen, J. M. He, Y. P. Bai and H. B. Zeng, *J. Colloid Interface Sci.*, 2021, **585**, 420-432.

23. S. S. Wu, Z. J. Shao, H. Xie, T. Xiang and S. B. Zhou, *J. Mater. Chem. A*, 2021, **9**,1048-1061.

24. Q. Chen, L. Feng, H. T. Cheng, Y. L. Wang, H. Wu, T. Xu, W. F. Zhao and C. S. Zhao, *J. Mater. Chem. B*, 2021, https://doi.org/10.1039/D1TB00019E.

25. F. F. Fu, Z. Y. Chen, H. Wang, C. H. Liu, Y. X. Liu and Y. J. Zhao, *Nanoscale,* 2019, **11**, 10846-10851.

26. F. Zhao, Y. Shi, L. J. Pan and G. H. Yu, *Acc. Chem. Res.*, 2017, **50**, 1734-1743.

27. Y. S. Zhang and A. Khademhosseini, *Science*, 2017, **500**, 356.

28. Y. F. Luo, W. L. Li, Q. Y. Lin, F. L. Zhang, K. He, D. P. Yang, X. J. Loh and X. D. Chen, *Adv. Mater.,* 2021, 2007848.

29. T. Xu, D. Z. Yang, S. Y. Zhang, T. Y. Zhao, M. Zhang and Z. Z. Yu, *Carbon*, 2021, **171**, 201-210.

30. B. Blanco-Fernandez, V. M. Gaspar, E. Engel and J. F. Mano, *Adv. Sci.*, 2021, **8**, 2003129.

31. S. Hinderer, S. L. Layland and K. Schenke-Layland, *Adv. Drug. Deliv. Rev.*, 2016, **97**, 260-269.

32. C. Zhang, Y. S. Zhou, H. J. Han, H. X. Zheng, W. H. Xu and Z. K. Wang, *ACS Nano*, 2021, **15**, 1785-1794.

33. A. Khademhosseini and R. Langer, *Biomaterials*, 2007, **28**, 5087-5092.

34. J. Liu, S. T. Lin, X. Y. Liu, Z. Qin, Y. Y. Yang, J. F. Zang and X. H. Zhao, *Nat. Commun.,* 2020, **11**, 1071.

35. Z. Ma, W. Shi, K. Yan, L. J. Pan and G. H. Yu, *Chem. Sci.*, 2019, **10**, 6232-6244.

36. W. Zhang, J. Ma, W. J. Zhang, P. G. Zhang, W. He, J. Chen and Z. M. Sun, *Nanoscale*, 2020, **12**, 6637-6643.

37. Y. J. Peng, M. H. Pi, X. L. Zhang, B. Yan, Y. S. Li, L. Y. Shi and R. Ran, *Polymer*, 2020, 122469.

38. D. L. Gan, T. Shuai, X. Wang, Z. Q. Huang, F. Z. Ren, L. M. Fang, K. F. Wang, C. M. Xie and X. Lu, *Nano-Micro Lett.,* 2020, **12**, 169.

39. H. W. Zhou, Z. W. Wang, W. F. Zhao, X. M. Tong, X. L. Jin, X. C. Zhang, Y. Yu, H. B. Liu, Y. C. Ma, S. S. Li and W. X. Chen, *Chem. Eng. J.*, 2021, **403**, 126307.

40. Y. J. Ma, K. I. Jang, L. Wang, H. N. Jung, J. W. Kwak, Y. G. Xue, H. Chen, Y. Y. Yang, D. W. Shi, X. Feng, J. A. Rogers and Y. G. Huang, *Adv. Funct. Mater.*, 2016, **26**, 5345-5351.

41. D. Mawad, A. Lauto and G. G. Wallace, Conductive Polymer Hydrogels. Polymeric Hydrogels as Smart Biomaterials, 2016, 19-45.

42. V. R. Feig, H. Tran, M. Lee, K. Liu, Z. J. Huang, L. Beker, D. G. Mackanic and Z. N. Bao, *Adv. Mater.,* 2019, **31**, 1902869.

43. S. Sekine, Y. Ido, T. Miyake, K. Nagamine and M. Nishizawa, *J. Am. Chem. Soc.*, 2010, **132**, 13174-13175.

44. H. Nurly, Q. Yan, B. Song and Y. Shi, *Eur. Polym. J.*, 2019, **110**, 114-122.

45. J. J. Wei, J. J. Xie, P. C. Zhang, Z. Y. Zou, H. Ping, W. M. Wang, H. Xie, J. Z. Shen, L. W. Lei and Z. Y. Fu, *ACS Appl. Mater. Interfaces,* 2021, **13**, 2952-2960.

46. W. S. Yang, M. F. Pan, C. Huang, Z. Q. Zhao, J. M. Wang and H. B. Zeng, *Compos. Commun.,* 2021, **24**, 100645.

47. D. Trucco, L. Vannozzi, E. Teblum, M. Telkhozhayeva, G. D. Nessim, S. Affatato, H. AlHaddad, G. Lisignoli and L. Ricotti, *Adv. Healthcare Mater.*, 2021, 2001434.

48. Y. Wang, G. H. Gao and X. Y. Ren, *Polymer,* 2021, **215**, 123340.

49. M. Ahmadi, D. Monji and F. A. Taromi, *Soft Matter*, 2021, **17**, 955-964.

50. X. Zhao, F. Chen, Y. H. Li, H. Lu, N. Zhang and M. M. Ma, *Nat. Commun.,* 2018, **9**, 3579.

51. X. S. Li, F. Liu, D. P. Huang, N. Xue, Y. Y. Dang, M. Q. Zhang, L. L. Zhang, B. Li, D. Liu, L.Wang, H. Liu and X. T. Tao, *Adv. Funct. Mater.*, 2020, **24**, 2000308.

52. X. Sun, F. L. Yao and J. J. Li, *J. Mate. Chem. A*, 2020, **8**, 18605-18623.

53. H. Y. Nyein, W. Gao, Z. Shahpar, S. Emaminejad, S. Challa, K. Chen, H. M. Fahad, L. C. Tai, H. Ota, R. W. Davis and A. Javey, *ACS Nano*, 2016, **10**, 7216-7224.

54. Y. Onuki, M. Nishikawa, M. Morishita and K. Takayama, *Int. J. Pharm.*, 2008, **349**, 47-52.

55. A. Li, Y. Jia, S. Sun, Y. Xu, B. B. Minsky, M. A. C. Stuart, H. Colfen, R. von Klitzing and X. Guo, *ACS Appl. Mater. Interfaces*, 2018, **10**, 10471-10479.

56. T. S. Sonia, P. A. Mini, R. Nandhini, K. Sujith, B. Avinash, S. V. Nair and K. P. V. *Bull. Mater. Sci.*, 2013, **36**, 547-551.

57. H. Y. Y. Nyein, M. Bariya, L. Kivimäki, S. Uusitalo, T. S. Liaw, E. Jansson, C. H. Ahn, J. A. Hangasky, J. Zhao, Y. Lin, T. Happonen, M. Chao, C. Liedert, Y. Zhao, L. C. Tai, J. Hiltunen, A. Javey. *Sci. Adv.*, **2019**, 5, 9906.

58. Y. Lu, K. Jiang, D. Chen, G. Shen, *Nano Energy*, **2019**, 58, 624-632.

59. Q. Cao, B. Liang, X. Mao, J. Wei, T. Tu, L. Fang, X. Ye, *Electroanalysis*, **2021**, 33, 643-651.